Isolating Degradation Mechanisms in Mixed Emissive Layer Organic Light-Emitting Devices

John S. Bangsund, Kyle W. Hershey, and Russell J. Holmes*

Department of Chemical Engineering and Materials Science, University of Minnesota, Minneapolis, Minnesota 55455, United States

S *Supporting Information*

ABSTRACT: Degradation in organic light-emitting devices (OLEDs) is generally driven by reactions involving excitons and polarons. Accordingly, a common design strategy to improve OLED lifetime is to reduce the density of these species by engineering an emissive layer architecture to achieve a broad exciton recombination zone. Here, the effect of exciton density on device degradation is analyzed in a mixed host emissive layer (M-EML) architecture which exhibits a broad recombination zone. To gain further insight into the dominant degradation mechanism, losses in the exciton formation efficiency and photoluminescence (PL) efficiency are decoupled by tracking the emissive layer PL during device degradation. By varying the starting luminance and M-EML thickness, the rate of PL degradation is found to depend strongly on recombination zone width and hence exciton density. In contrast, losses in the exciton formation depend only weakly on the recombination zone, and thus may originate outside of the emissive layer. These results suggest that the lifetime enhancement observed in the M-EML architectures reflects a reduction in the rate of PL degradation. Moreover, the varying roles of excitons and polarons in degrading the PL and exciton formation efficiencies suggest that kinetically distinct pathways drive OLED degradation and that a single degradation mechanism cannot be assumed when attempting to model the device lifetime. This work highlights the potential to extract fundamental insight into OLED degradation by tracking the emissive layer PL during lifetime testing, while also enabling diagnostic tests on the root causes of device instability.

KEYWORDS: photoluminescence, exciton formation, degradation, exciton quenchers, recombination zone, OLEDs
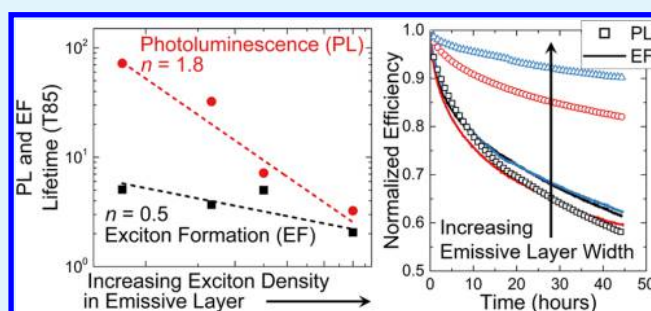
1. INTRODUCTION

Improving operational stability is one of the key challenges facing further commercial development of organic light-emitting devices (OLEDs) for large-area displays and solid-state lighting applications.[1] Previous work has shown that intrinsic degradation in OLEDs is driven by chemical reactions mediated by both excited molecules (excitons) and charged molecules (polarons).[1−6] One general strategy to improve lifetime, therefore, is to reduce the density of these species by expanding the exciton recombination zone (RZ). A broad RZ can be achieved by engineering the emissive layer architecture to balance charge transport and injection. To this end, graded- and step-doping profiles,[7−10] mixtures and gradients of multiple host materials,[11−18] and double emissive layers[19−21] have been shown to yield a broad and centered RZ and consequently to improve exciton confinement, charge balance, efficiency, and lifetime. Here, we study degradation in a mixed host emissive layer (M-EML) architecture, in which hole- and electron-transport materials are uniformly mixed with an emissive guest. The use of a mixed emissive layer has been shown to reduce the roll-off in the external quantum efficiency observed under high current injection and increase the lifetime. Indeed, while a favorable trend between the device lifetime and the RZ width has been well-documented,[7,8,16,22,23] the specific role the RZ

plays in degradation kinetics remains an active area of investigation. Prior work has proposed that the RZ, by establishing charge and exciton densities, plays a role in determining the formation of both exciton quenchers and nonradiative recombination centers.[2,7]

In this work, the overall degradation in device electroluminescence (EL) is decoupled in terms of corresponding reductions in the efficiencies of exciton formation (η_{EF}) and radiative recombination (i.e., photoluminescence (PL) efficiency, η_{PL}).[24−28] Specifically, we find that a systematic increase in the RZ width for an M-EML OLED leads to a sharp reduction in the rate of degradation of η_{PL}. The exciton formation efficiency is less sensitive to reductions in the M-EML width, suggesting that the exciton density may not as strongly dictate degradation in η_{EF}, potentially indicating a greater role for factors outside the emissive layer. These results provide diagnostic insight into the source of device instability and reveal new details regarding the kinetics of degradation.

2. THEORY

During constant current operation, losses in EL intensity occur because of reductions in the external quantum efficiency (η_{EQE}), which can be expressed as[28,29]

$$\eta_{EQE} = \chi\eta_{EF}\eta_{PL}\eta_{OC}\eta_\tau \tag{1}$$

where χ is the spin fraction, η_{OC} is the outcoupling efficiency, and η_τ is the fraction of excitons that recombine via the natural lifetime, representing the degree of bimolecular quenching at a given current density.[28,30] Here, we replace the conventional charge balance factor, γ, with a more general exciton formation efficiency, η_{EF}. Charge balance is typically cast as the efficiency of charge carrier recombination in the emissive layer, competing with carrier leakage.[1,31] In contrast, we take η_{EF} to represent the efficiency of forming excitons on an emissive molecule, which can be reduced by both introduction of nonradiative recombination centers and charge leakage.[2,32]

It has previously been argued that η_{PL} and η_{EF} will be the primary contributors to luminance loss,[1,26] whereas χ, η_{OC}, and η_τ will only vary negligibly during device degradation.[28] Changes in η_{OC} could occur in the event of significant shifts in the RZ position, but the broad RZ present in M-EML devices reduces this effect. In addition, η_τ is expected to increase during degradation because of the reduced exciton density. Previous work has found, however, that this increase is small unless testing above 10 000 cd/m^2.[28] The potential error introduced by these simplifying assumptions is discussed at the end of this work and in the Supporting Information. Therefore, at any point during the degradation, the normalized device EL can be written as

$$\frac{\eta_{EQE}(t)}{\eta_{EQE}(t=0)} = \frac{\eta_{EF}(t)}{\eta_{EF}(t=0)}\frac{\eta_{PL}(t)}{\eta_{PL}(t=0)} \tag{2}$$

Equation 2 suggests that a simultaneous measurement of device EL (yielding η_{EQE}) and PL (yielding η_{PL}) permits the extraction of the exciton formation efficiency as a function of time. The direct connection between the PL intensity and η_{PL} assumes that the absorption of the emissive layer is constant, changes in the PL intensity come from an increase in the nonradiative rate, and there is substantial overlap between the RZ and the optically generated exciton profile. Previous work found a direct correspondence between the reduction in the PL intensity and the exciton lifetime with degradation,[28] supporting the first two assumptions. The validity of the latter assumption is discussed at the end of this work.

3. EXPERIMENTAL METHODS

OLEDs with active areas of 25 mm^2 were fabricated on glass substrates prepatterned with a 150 nm thick anode layer of indium tin oxide (Xinyan). Substrates were solvent-cleaned and exposed to UV−ozone ambient. The devices consisted of a 60 nm thick hole-injection layer (HIL) of poly(thiophene-3-[2[(2-methoxyethoxy)ethoxy]-2,5-diyl) (AQ1200, Sigma-Aldrich), a 4,4′,4″-tris(N-carbazolyl)triphenylamine (TCTA, TCI America) hole-transport layer (HTL), an M-EML consisting of a 47.5 vol % TCTA, 47.5 vol % 2,2′,2″(1,3,5-benzenetriyl)tris-(1-phenyl-1H-benzimidazole) (TPBi, Lumtec), and 5 vol % of the green phosphorescent emitter fac-tris(2-phenylpyridine)iridium(III) (Ir(ppy)$_3$, Lumtec), a TPBi electron-transport layer (ETL), and a LiF (1 nm)/Al (100 nm) cathode. When varying the M-EML thickness (10, 30, and 60 nm), the HTL and ETL thicknesses are varied equally to maintain a total device thickness of 100 nm. The HIL is spin-cast in a N$_2$ glovebox and annealed for 30

min at 150 °C. The remaining layers are deposited by vacuum thermal evaporation at a base pressure <7 × 10^{-7} Torr and a rate of 0.3 nm/s.

Efficiency measurements were taken with an Agilent 4155C parameter analyzer and a large-area photodiode (Hamamatsu S3584-08). EL spectra were collected with an Ocean Optics HR4000 spectrometer.

The electrically generated exciton profile (i.e., the RZ) of the 60 nm thick M-EML was measured using a sensitizer doping method, as described previously,[7,12] with 2 nm thick strips doped with 2 vol % platinum tetraphenyl-tetrabenzoporphine (PtTPTBP) centered at 5, 15, 30, 45, and 55 nm from the HTL. Inclusion of the strip had a negligible impact on the device current density−voltage characteristics (shown in Figure S1). The RZ was extracted from the EL spectra by normalizing the photon flux emitted from each sensitizer strip by the spectrally weighted outcoupling efficiency for the PtTPTBP emission at that position in the device.

During degradation of the M-EML devices, the decay in PL from the emissive layer is collected in tandem with EL by intermittently turning off the applied current and illuminating the device with a λ = 405 nm continuous-wave (CW) laser (Coherent OBIS LX). The CW laser is incident at an angle of 45°, and the PL is collected through a λ = 450 nm long-pass filter to prevent the detection of scattered pump laser light. The pump wavelength is chosen so that only the emissive guest is excited. The laser spot diameter is ~1 mm and hence averages over ~3% of the total device area. Current is applied for 10 min between the PL measurements, which take ~20 s. This intermittency in current has no discernible effect on the degradation rate, and no laser-induced degradation was observed after over 500 repetitions of the laser measurement cycle on a nonoperating device.

4. RESULTS AND DISCUSSION

4.1. RZ and Device Characteristics. To systematically study the effect of RZ width on degradation, we selected an architecture (inset in Figure 1c) with an RZ which spans the entire emissive layer,[33] allowing the M-EML thickness, d_{EML}, to be taken as a proxy for the RZ width. In principle, this permits the exciton density in the emissive layer to be tuned by changing d_{EML}. The current density−voltage−luminance characteristics and external quantum efficiency for the devices with emissive layer thicknesses of 10, 30, and 60 nm are shown in Figure 1. As d_{EML} is increased from 10 to 60 nm, the peak efficiency increases gradually from (17 ± 1) to (19 ± 2)% and the onset of the efficiency roll-off is pushed to higher current densities (Figure 1c). This change in the roll-off is consistent with an increase in the RZ width, which leads to a reduced exciton density and reduced severity of bimolecular quenching processes.[34,35]

To experimentally confirm that the RZ spans the majority of the M-EML in this architecture, we used a sensitizer-doped strip approach.[7,12] The EL spectra of the sensitized devices are shown in Figure 2a. The outcoupling of the PtTPTBP emission, calculated using an optical transfer matrix and a power dissipation model (shown in Figure 2b),[36−38] drops by a factor of 3 across the emissive layer. Normalizing the sensitizer EL by the outcoupling profile, the exciton density is found to remain above 60% of the peak across the entire 60 nm M-EML at a current density of 10 mA/cm^2 (Figure 2c). As the current density increases from 0.1 to 10 mA/cm^2, the peak of the RZ migrates from the ETL side to the HTL side of the M-EML. These findings are consistent with other reports for similar device architectures[12,33] and confirm that d_{EML} is a good proxy for the RZ width.

4.2. Lifetime Scaling with the RZ and Luminance. The reduction in the device EL over time is shown in Figure 3a for the devices having emissive layer thicknesses of 10, 30, or 60 nm at an initial luminance of L_0 = 3000 cd/m^2, with the
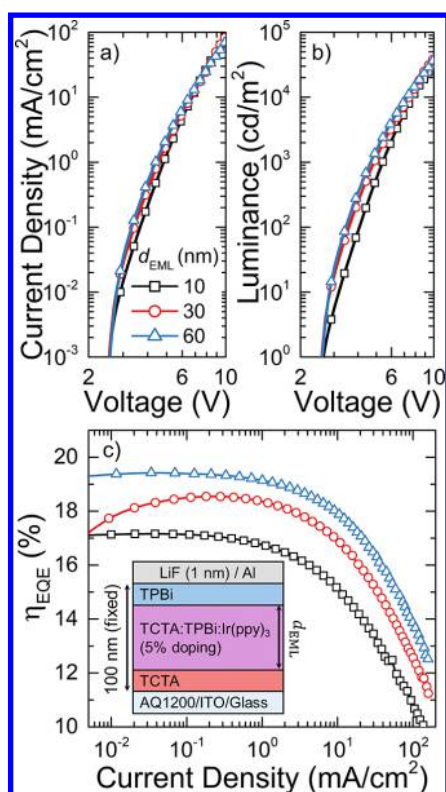
Figure 1. (a) Current density vs voltage, (b) luminance vs voltage, and (c) external quantum efficiency (η_{EQE}) vs current density for devices with M-EML thicknesses (d_{EML}) of 10, 30, and 60 nm. Inset: Device architecture of interest.

Figure 2. (a) EL spectra for sensitized devices with d_{EML} = 60 nm at a current density of 1 mA/cm^2. Sensitizer-doped strips are centered at 5, 15, 30, 45, and 55 nm from the HTL. (b) Electric field profile of the PL pump (λ = 405 nm, incident angle = 45°) and the spectrally weighted outcoupling efficiency for Ir(ppy)$_3$ emission. (c) Normalized exciton density profiles for 0.1, 1, and 10 mA/cm^2. Solid lines are guides to the eye. Error bars in position represent the width of the dopant strips and the Förster radius between Ir(ppy)$_3$ and PtTPTBP (3.7 nm). Error bars in relative exciton density represent standard deviations taken from a minimum of four samples.

corresponding decays in PL and η_{EF} shown in Figure 3b. The EL lifetime increases by approximately a factor of 3 in increasing the thickness from 10 to 60 nm, and nearly all this enhancement can be attributed to a reduced rate of PL degradation. No trend with the thickness is apparent in the η_{EF} decays shown in Figure 3b, which are all within a typical device-to-device variation. In contrast, the PL decays show a dramatic separation with the thickness. We also note that a reduction in η_{EF} dominates the overall degradation rate in the 30 and 60 nm thick M-EML devices but is comparable to the PL losses in the 10 nm M-EML device. These results suggest that the reduced degradation in the emissive layer PL efficiency may be the primary reason for the enhanced stability in the M-EML architectures, as compared to their single-host counterparts with narrower RZs. Moreover, the combination of an improved efficiency roll-off and PL lifetime with an increased RZ width, and thus decreased exciton density, provides further evidence of a link between exciton quenching events and the degradation of PL efficiency.[6] Losses in η_{EF}, however, appear to be relatively insensitive to exciton density.

To further confirm the link between the exciton density and the PL loss, the exciton density was approximately matched between these architectures by scaling the starting luminance by the ratio of the M-EML thicknesses. Shown in Figure 4, the PL degradation is nearly identical for devices with d_{EML} = 10, 30, and 60 nm operated at luminances of 1000, 3000, and 6000 cd/m^2, respectively. The exciton formation efficiency losses, on the other hand, are rapidly accelerated as luminance is increased. At long times, the PL degradation slows down slightly with increasing M-EML thickness, and this is attributed to the large differences in the exciton formation efficiency

losses. The exciton density does not remain matched over the course of the entire test because of these differences in η_{EF} losses, and consequently, the formation rate for the exciton quenchers will be reduced at long times in the devices with larger d_{EML}. This observation of matched PL losses under a scaled luminance has been reproduced under a range of scaled luminances from 330 to 15 000 cd/m^2 (Figure S2). Despite comparable exciton densities in the emissive layer, the exciton formation efficiency losses differ substantially and appear to scale with increased luminance and current density. The increased current density would result in a larger polaron density in the transport layers and could lead to an increase in the rate of defect formation mediated by unstable cationic or anionic molecules.[6] Alternatively, the trend with luminance could be explained as an increase in interfacial photo-degradation of the cathode or anode because of the device EL.[39−41]

To further validate the results in Figure 3, the degradation behavior of these devices was measured across a range of initial luminances. Because the RZ spans the entire M-EML thickness, as demonstrated in section 4.1, the exciton density at a given luminance is inversely proportional to the EML thickness ($N \propto 1/d_{EML}$). In this sense, tuning the thickness of the M-EML is analogous to accelerated aging under an increased initial luminance and might be expected to show a similar scaling relationship. OLED lifetime has been widely observed to follow a $1/L_0^n$ relationship,[42] where L_0 is the initial luminance and n is
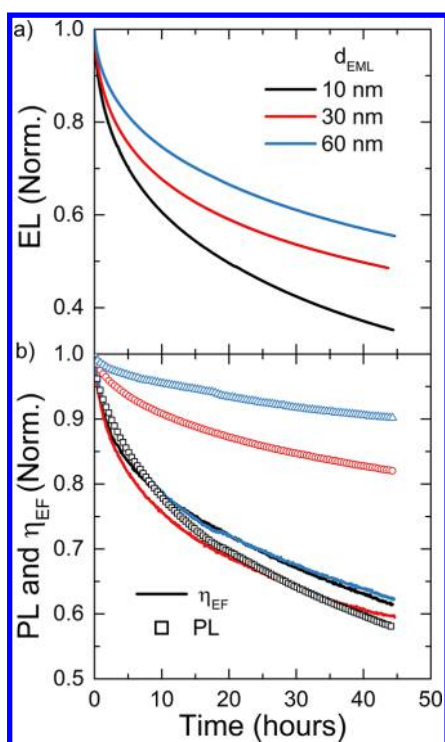
Figure 3. (a) Normalized EL intensity for 10, 30, and 60 nm M-EML devices operated at an initial luminance of 3000 cd/m^2. The current densities for these tests were 7.2, 6.4, and 6.0 mA/cm^2, respectively. (b) Decoupled PL(symbols) and exciton formation efficiency losses (η_{EF}, solid lines) corresponding to the curves in (a).
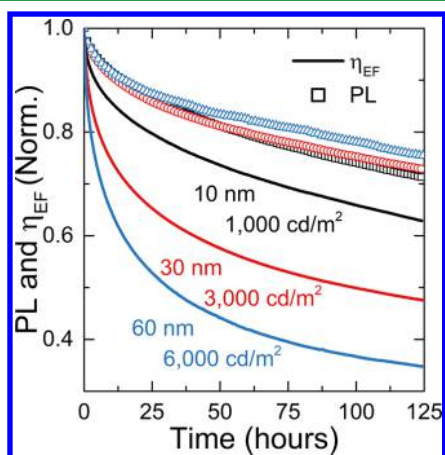
Figure 4. Decoupled losses in PL (symbols) and η_{EF} (solid lines) for 10, 30, and 60 nm M-EML devices operated at initial luminances of 1000, 3000, and 6000 cd/m^2, respectively. The current densities for these tests were 2.0, 6.0, and 12.0 mA/cm^2, respectively. Scaling the initial luminance by the emissive layer thickness results in an approximately matched exciton density and similar timescales for the PL loss.

a device-specific parameter typically between 1 and 2. For these devices, $n = 1.8 \pm 0.1$ for the t_{50} of EL and is independent of the M-EML thickness (Figure S3). As shown in Figure 5a, the degradations in PL and η_{EF} for a 60 nm M-EML show a similar acceleration behavior as a function of luminance, with $n = 1.8$ and $n = 1.75$, respectively. Comparable slopes are seen for 10 and 30 nm M-EML devices (see Figure S3).

However, when scaled by $1/d_{EML}$, as displayed in Figure 5b, η_{EF} and PL show a distinct scaling behavior. While PL t_{85} shows

a slope of $n = 1.9 \pm 0.3$, almost identical to the slope under luminance acceleration, $\eta_{EF}\, t_{85}$ shows a much shallower slope of $n = 0.5 \pm 0.2$ (decreasing to $n = 0.3 \pm 0.3$ at 10 000 cd/m^2). This raises several important implications. First, the nearly identical slopes for PL in Figure 5a,b provide further evidence that PL losses in this system are determined by the exciton density and the width of the RZ and imply that there is a direct scaling law between the RZ width and the PL lifetime. While polarons can generally play a role in the PL degradation,[27,43] it is unlikely that polaron density scales identically with both luminance and d_{EML}, implying that the degradation may be dominated by a single-exciton driven or an exciton−exciton annihilation-driven degradation mechanism in this system. Second, the shallow dependence of $\eta_{EF}\, t_{85}$ on the RZ width (and hence exciton density) shown in Figure 5b suggests that excitons play a less significant role in the η_{EF} degradation. Notably, the difference in scaling with L_0 and d_{EML} for $\eta_{EF}\, t_{85}$ suggests that multiple degradation mechanisms comprise the total η_{EF} loss.

The exciton formation loss is typically attributed to the accumulation of nonradiative recombination centers in the emissive layer[4,32,44] and has been linked to the exciton−polaron interactions.[26] We interpret the d_{EML}-dependent increase in the η_{EF} degradation (Figure 5b) to reflect the generation of nonradiative recombination centers by an exciton-mediated process consistent with these reports. However, this mechanism alone cannot account for the degradation in η_{EF}, as the scaling with L_0 is much steeper (Figure 5a). This contrasting behavior suggests that a second mechanism which is independent of the emissive-layer exciton density governs η_{EF} losses. As discussed above, this behavior is consistent with degradation mediated primarily by polarons or photodegradation of the cathode or anode interface[39−41] and thus may originate outside of the emissive layer.

These findings have implications for efforts to model OLED lifetime. Previous modeling attempts have often assumed that the same defect population responsible for exciton quenching was also responsible for the nonradiative recombination of charge carriers and that this population resided entirely in the emissive layer.[2,7] Defect populations external to the emissive layer have been considered but only for the purposes of fitting the voltage rise.[45] Other work has argued that triplet-polaron quenching increases during degradation because of the trapped charge in the emissive layer.[46] In all cases, the generation of defects is proposed to proceed via bimolecular quenching processes, either triplet−triplet annihilation or triplet-polaron quenching.[47] While these treatments have yielded reasonable fits of the overall degradation behavior, they are unable to capture the behavior observed here. The exciton formation and PL degradation would be expected to trend together within these formalisms, whereas Figure 5b shows a clearly distinct scaling behavior. Our results thus show that losses to η_{PL} and η_{EF} originate from kinetically distinct mechanisms. Moreover, the weak dependence of η_{EF} on the exciton density indicates that the defects external to the emissive layer may play an important role in luminance loss and should be considered in future modeling attempts.

It is important to note that defects that serve as nonradiative recombination centers could have suitable energetics to serve as exciton quenchers and vice versa.[1] However, the differing scaling behavior observed here indicates that the exciton quenchers formed in the EML are likely inefficient nonradiative recombination centers for charge carriers.
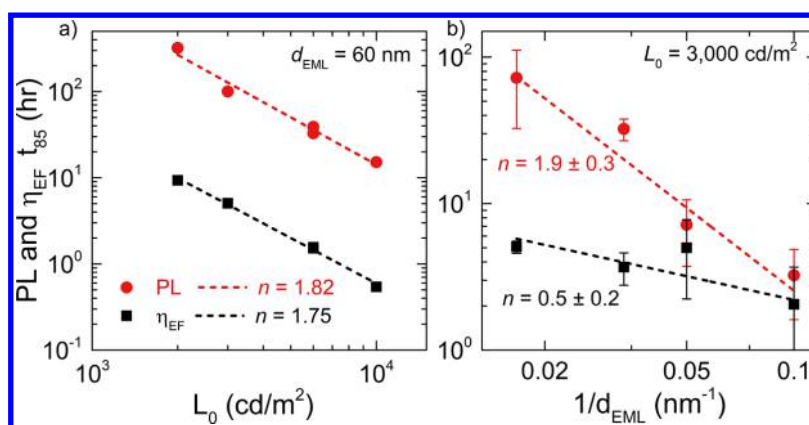
Figure 5. (a) Time to 85% of the initial value (t_{85}) for PL and η_{EF} plotted against initial luminance for the 60 nm M-EML. The acceleration factor, n, is approximately 1.8 in both cases. (b) t_{85} for PL and η_{EF} plotted against $1/d_{EML}$ for devices tested at an initial luminance of 3000 cd/m². A similar power law relationship is observed, and the analogous acceleration factor is $n = 1.9 \pm 0.3$ for PL, nearly identical to the luminance acceleration factor. For η_{EF}, a much shallower factor of $n = 0.5 \pm 0.2$ is observed, suggesting a separate degradation mechanism. Error bars represent standard deviations calculated over at least four measurements across at least two separate device sets.

4.3. Analysis of Measurement Error. In extracting η_{EF}, we assume that the measured PL intensity is representative of the device-relevant η_{PL} which helps determine the EL efficiency (eq 1). This assumption may begin to break down in wide emissive layer architectures in which the optically and electrically generated exciton profiles are challenging to match.[26,44] In such cases, the measured PL intensity will be a convolution of the spatial dependences of the RZ, the electric field profile of the $\lambda = 405$ nm pump, and the outcoupling efficiency. The dependence of outcoupling on the position for Ir(ppy)$_3$ and PtTPTBP emissions and the electric field profile of the $\lambda = 405$ nm pump at 45° from the normal incidence were calculated using an optical transfer matrix and a power dissipation model (shown in Figure 2b).[36−38] As shown in Figure 2b,c, the RZ and $\eta_{OC}(x)$ of Ir(ppy)$_3$ peak on the HTL side of the emissive layer, and the electric field profile of the pump peaks at 35 nm from the HTL. Qualitatively, the substantial overlap of these profiles suggests that errors may be minimal in these devices.

To quantify the measurement error introduced by this mismatch, we employ a basic defect quenching model, similar to the treatment of Giebink et al.,[2] and compare our measured PL loss with the device-relevant η_{PL} loss. By assuming a unimolecular (single-exciton-induced) defect formation process, we find that the PL measurement underestimates the actual η_{PL} loss by <1% for degradation up to PL/PL$_0$ = 85%. In the case of a bimolecular process (i.e., exciton−exciton annihilation-induced defect formation), the error remains <3% up to PL/PL$_0$ = 85%. It is worth noting that the model used here does not consider the possibility of a large transfer radius between the defect and Ir(ppy)$_3$, which would likely serve to broaden the effective defect profile and hence reduce the measurement error. These error estimates, therefore, represent upper bounds and are within typical device-to-device variations. Nonetheless, this analysis underscores the importance of considering the optical design of a device architecture before attempting to quantitatively decouple PL and η_{EF} losses. More detailed discussion of these calculations can be found in the Supporting Information (Figure S4).

We also consider the accuracy of the assumption that η_{OC} is constant during degradation. In the absence of changes in optical constants, molecular orientation, or substantial crystallization, the primary mechanism for the η_{OC} loss is the RZ

migration.[1] The evidence of RZ migration during degradation has been observed in several cases[31,48] and is generally attributed to the changes in injection properties on either side of the EML.[40] While we do not track the RZ position during degradation, we assess the limits of η_{OC} changes due to RZ movement. In the most extreme case, the RZ would be a delta function moving from the position of highest outcoupling efficiency (24.7%) to the lowest (15.3%) or vice versa, resulting in a 38% relative change in the outcoupling efficiency. In practice, the RZ will have a substantial width. We considered the error introduced by migrating a Gaussian RZ with full width at half maximum ranging from 10 to 60 nm. For a narrow RZ, η_{OC} could fall from 23 to 16% if the RZ fully migrated from the HTL side to the ETL side. For a wide RZ similar to that measured here, however, η_{OC} only falls from 23 to 22%. The losses to η_{OC} can therefore be neglected in devices with a narrow emissive layer or a broad RZ. These calculations are discussed in more detail in the Supporting Information (Figure S5).

Finally, we revisit the assumption that changes to η_τ are negligible. By employing a bimolecular quenching model and previously measured rate constants,[30] we find that η_τ increases 2.7% by 50% of the initial luminance (EL t_{50}) for a 10 nm M-EML operated at 3000 cd/m² (Figure S6). This effect is reduced in devices with a thicker d_{EML} because of the lower initial exciton density but is not large enough to alter the conclusions of this work.

5. CONCLUSIONS

In conclusion, we find that broadening the RZ sharply reduces the rate of PL degradation, showing a similar scaling relationship as with the initial luminance variation and confirming that PL degradation is strongly dependent on the exciton density. However, losses in the exciton formation efficiency (η_{EF}) show a weaker dependence on the RZ width, suggesting that η_{EF} losses are less sensitive to exciton density and may partly originate outside of the M-EML in this system. Notably, the different dependences of PL and exciton formation efficiency loss on the RZ width provide clear evidence that kinetically distinct pathways drive OLED degradation and that a single degradation mechanism cannot be assumed when attempting to model the device lifetime.

These results highlight the capability of decoupled measurements of PL and η_{EF} losses to yield useful diagnostic insight into the source of device instability and shed light on the kinetics of degradation and the nature of defects.

■ ASSOCIATED CONTENT

ⓢ Supporting Information

The Supporting Information is available free of charge on the ACS Publications website at DOI: 10.1021/acsami.7b16643.

> Influence of sensitizer strips on electrical characteristics; luminance dependence of EL, PL, and exciton formation; additional lifetime data; and calculations regarding sources of measurement errors (PDF)

■ AUTHOR INFORMATION

Corresponding Author

*E-mail: rholmes@umn.edu.

ORCID ⓘ

Russell J. Holmes: 0000-0001-7183-3673

Notes

The authors declare the following competing financial interest(s): R.J.H. is a member of The Dow Chemical Company Technical Advisory Board.

■ ACKNOWLEDGMENTS

■ REFERENCES

(1) Scholz, S.; Kondakov, D.; Lüssem, B.; Leo, K. Degradation Mechanisms and Reactions in Organic Light-Emitting Devices. *Chem. Rev.* **2015**, *115*, 8449−8503.

(2) Giebink, N. C.; D'Andrade, B. W.; Weaver, M. S.; Mackenzie, P. B.; Brown, J. J.; Thompson, M. E.; Forrest, S. R. Intrinsic Luminance Loss in Phosphorescent Small-Molecule Organic Light Emitting Devices due to Bimolecular Annihilation Reactions. *J. Appl. Phys.* **2008**, *103*, 044509.

(3) Giebink, N. C.; D'Andrade, B. W.; Weaver, M. S.; Brown, J. J.; Forrest, S. R. Direct Evidence for Degradation of Polaron Excited States in Organic Light Emitting Diodes. *J. Appl. Phys.* **2009**, *105*, 124514.

(4) So, F.; Kondakov, D. Degradation Mechanisms in Small-Molecule and Polymer Organic Light-Emitting Diodes. *Adv. Mater.* **2010**, *22*, 3762−3777.

(5) Zhang, Y.; Aziz, H. Influence of the Guest on Aggregation of the Host by Exciton−Polaron Interactions and Its Effects on the Stability of Phosphorescent Organic Light-Emitting Devices. *ACS Appl. Mater. Interfaces* **2016**, *8*, 14088−14095.

(6) Schmidbauer, S.; Hohenleutner, A.; König, B. Chemical Degradation in Organic Light-Emitting Devices: Mechanisms and Implications for the Design of New Materials. *Adv. Mater.* **2013**, *25*, 2114−2129.

(7) Zhang, Y.; Lee, J.; Forrest, S. R. Tenfold Increase in the Lifetime of Blue Phosphorescent Organic Light-Emitting Diodes. *Nat. Commun.* **2014**, *5*, 5008.

(8) Wu, Z.; Sun, N.; Zhu, L.; Sun, H.; Wang, J.; Yang, D.; Qiao, X.; Chen, J.; Alshehri, S. M.; Ahamad, T.; Ma, D. Achieving Extreme Utilization of Excitons by an Efficient Sandwich-Type Emissive Layer Architecture for Reduced Efficiency Roll-Off and Improved Opera-tional Stability in Organic Light-Emitting Diodes. *ACS Appl. Mater. Interfaces* **2016**, *8*, 3150−3159.

(9) Chin, B. D.; Suh, M. C.; Kim, M.-H.; Lee, S. T.; Kim, H. D.; Chung, H. K. Carrier Trapping and Efficient Recombination of Electrophosphorescent Device with Stepwise Doping Profile. *Appl. Phys. Lett.* **2005**, *86*, 133505.

(10) Lee, J. Y. 17.3: Study of Light Emission Mechanism and Long Lifetime in Phosphorescent Organic Light Emitting Diodes Using Graded Doping Structure. *SID Int. Symp. Dig. Tech. Pap.* **2006**, *37*, 1103−1105.

(11) Chwang, A. B.; Kwong, R. C.; Brown, J. J. Graded Mixed-Layer Organic Light-Emitting Devices. *Appl. Phys. Lett.* **2002**, *80*, 725−727.

(12) Erickson, N. C.; Holmes, R. J. Investigating the Role of Emissive Layer Architecture on the Exciton Recombination Zone in Organic Light-Emitting Devices. *Adv. Funct. Mater.* **2013**, *23*, 5190−5198.

(13) Han, T.-H.; Kim, Y.-H.; Kim, M. H.; Song, W.; Lee, T.-W. Synergetic Influences of Mixed-Host Emitting Layer Structures and Hole Injection Layers on Efficiency and Lifetime of Simplified Phosphorescent Organic Light-Emitting Diodes. *ACS Appl. Mater. Interfaces* **2016**, *8*, 6152−6163.

(14) Tsai, Y.-C.; Jou, J.-H. Long-Lifetime, High-Efficiency White Organic Light-Emitting Diodes with Mixed Host Composing Double Emission Layers. *Appl. Phys. Lett.* **2006**, *89*, 243521.

(15) Lee, J.-H.; Wu, C.-I.; Liu, S.-W.; Huang, C.-A.; Chang, Y. Mixed Host Organic Light-Emitting Devices with Low Driving Voltage and Long Lifetime. *Appl. Phys. Lett.* **2005**, *86*, 103506.

(16) Brown, C. T.; Kondakov, D. A New Generation of High-Efficiency Red-Emitting Electroluminescent Devices with Exceptional Stability. *J. Soc. Inf. Disp.* **2004**, *12*, 323−327.

(17) Choong, V.-E.; Shen, J.; Curless, J.; Shi, S.; Yang, J.; So, F. Efficient and Durable Organic Alloys for Electroluminescent Displays. *J. Phys. D: Appl. Phys.* **2000**, *33*, 760.

(18) Liu, S. W.; Huang, C. A.; Lee, J. H.; Yang, K. H.; Chen, C. C.; Chang, Y. Blue Mixed Host Organic Light Emitting Devices. *Thin Solid Films* **2004**, *453−454*, 312−315.

(19) Wellmann, P.; Hofmann, M.; Zeika, O.; Werner, A.; Birnstock, J.; Meerheim, R.; He, G.; Walzer, K.; Pfeiffer, M.; Leo, K. High-Efficiency P-I-N Organic Light-Emitting Diodes with Long Lifetime. *J. Soc. Inf. Disp.* **2005**, *13*, 393−397.

(20) Jeon, W. S.; Park, T. J.; Kim, S. Y.; Pode, R.; Jang, J.; Kwon, J. H. Low Roll-off Efficiency Green Phosphorescent Organic Light-Emitting Devices with Simple Double Emissive Layer Structure. *Appl. Phys. Lett.* **2008**, *93*, 063303.

(21) He, G.; Pfeiffer, M.; Leo, K.; Hofmann, M.; Birnstock, J.; Pudzich, R.; Salbeck, J. High-Efficiency and Low-Voltage P-i-n Electrophosphorescent Organic Light-Emitting Diodes with Double-Emission Layers. *Appl. Phys. Lett.* **2004**, *85*, 3911−3913.

(22) Chin, B. D. Enhancement of Efficiency and Stability of Phosphorescent OLEDs Based on Heterostructured Light-Emitting Layers. *J. Phys. D: Appl. Phys.* **2011**, *44*, 115103.

(23) Yook, K. S.; Jeon, S. O.; Joo, C. W.; Lee, J. Y. Correlation of Lifetime and Recombination Zone in Green Phosphorescent Organic Light-Emitting Diodes. *Appl. Phys. Lett.* **2009**, *94*, 093501.

(24) Sandanayaka, A. S. D.; Matsushima, T.; Adachi, C. Degradation Mechanisms of Organic Light-Emitting Diodes Based on Thermally Activated Delayed Fluorescence Molecules. *J. Phys. Chem. C* **2015**, *119*, 23845−23851.

(25) Popovic, Z. D.; Aziz, H.; Hu, N.-X.; Ioannidis, A.; dos Anjos, P. N. M. Simultaneous Electroluminescence and Photoluminescence Aging Studies of tris(8-Hydroxyquinoline) Aluminum-Based Organic Light-Emitting Devices. *J. Appl. Phys.* **2001**, *89*, 4673−4675.

(26) Zhang, Y.; Aziz, H. Degradation Mechanisms in Blue Phosphorescent Organic Light-Emitting Devices by Exciton−Polaron Interactions: Loss in Quantum Yield versus Loss in Charge Balance. *ACS Appl. Mater. Interfaces* **2017**, *9*, 636−643.

(27) Winter, S.; Reineke, S.; Walzer, K.; Leo, K. Photoluminescence Degradation of Blue OLED Emitters. *Proc. SPIE* **2008**, *6999*, 69992N.

(28) Hershey, K. W.; Suddard-Bangsund, J.; Qian, G.; Holmes, R. J. Decoupling Degradation in Exciton Formation and Recombination

during Lifetime Testing of Organic Light-Emitting Devices. *Appl. Phys. Lett.* **2017**, *111*, 113301.

(29) Baldo, M. A.; O'Brien, D. F.; You, Y.; Shoustikov, A.; Sibley, S.; Thompson, M. E.; Forrest, S. R. Highly Efficient Phosphorescent Emission from Organic Electroluminescent Devices. *Nature* **1998**, *395*, 151−154.

(30) Hershey, K. W.; Holmes, R. J. Unified Analysis of Transient and Steady-State Electrophosphorescence Using Exciton and Polaron Dynamics Modeling. *J. Appl. Phys.* **2016**, *120*, 195501.

(31) Coburn, C.; Forrest, S. R. Effects of Charge Balance and Exciton Confinement on the Operational Lifetime of Blue Phosphorescent Organic Light-Emitting Diodes. *Phys. Rev. Appl.* **2017**, *7*, 041002.

(32) Kondakov, D. Y.; Sandifer, J. R.; Tang, C. W.; Young, R. H. Nonradiative Recombination Centers and Electrical Aging of Organic Light-Emitting Diodes: Direct Connection between Accumulation of Trapped Charge and Luminance Loss. *J. Appl. Phys.* **2003**, *93*, 1108−1119.

(33) Yook, K. S.; Lee, J. Y. Recombination Zone Study of Phosphorescent Organic Light-Emitting Diodes with Triplet Mixed Host Emitting Structure. *J. Ind. Eng. Chem.* **2010**, *16*, 181−184.

(34) Reineke, S.; Walzer, K.; Leo, K. Triplet-Exciton Quenching in Organic Phosphorescent Light-Emitting Diodes with Ir-Based Emitters. *Phys. Rev. B: Condens. Matter Mater. Phys.* **2007**, *75*, 125328.

(35) Erickson, N. C.; Holmes, R. J. Engineering Efficiency Roll-Off in Organic Light-Emitting Devices. *Adv. Funct. Mater.* **2014**, *24*, 6074−6080.

(36) Furno, M.; Meerheim, R.; Thomschke, M.; Hofmann, S.; Lüssem, B.; Leo, K. Outcoupling Efficiency in Small-Molecule OLEDs: From Theory to Experiment. *Proc. SPIE* **2010**, *7617*, 761716.

(37) Furno, M.; Meerheim, R.; Hofmann, S.; Lüssem, B.; Leo, K. Efficiency and Rate of Spontaneous Emission in Organic Electroluminescent Devices. *Phys. Rev. B: Condens. Matter Mater. Phys.* **2012**, *85*, 115205.

(38) Pettersson, L. A. A.; Roman, L. S.; Inganäs, O. Modeling Photocurrent Action Spectra of Photovoltaic Devices Based on Organic Thin Films. *J. Appl. Phys.* **1999**, *86*, 487−496.

(39) Wang, Q.; Aziz, H. Role of the Cathode Interfacial Layers in Improving the Stability of Organic Optoelectronic Devices. *Proc. SPIE* **2012**, *8476*, 84760D.

(40) Wang, Q.; Luo, Y.; Aziz, H. Photodegradation of the Organic/metal Cathode Interface in Organic Light-Emitting Devices. *Appl. Phys. Lett.* **2010**, *97*, 063309.

(41) Wang, Q.; Williams, G.; Aziz, H. Photo-Degradation of the Indium Tin Oxide (ITO)/organic Interface in Organic Optoelectronic Devices and a New Outlook on the Role of ITO Surface Treatments and Interfacial Layers in Improving Device Stability. *Org. Electron.* **2012**, *13*, 2075−2082.

(42) Meerheim, R.; Walzer, K.; Pfeiffer, M.; Leo, K. Ultrastable and Efficient Red Organic Light Emitting Diodes with Doped Transport Layers. *Appl. Phys. Lett.* **2006**, *89*, 061111.

(43) Song, W.; Lee, J. Y. Degradation Mechanism and Lifetime Improvement Strategy for Blue Phosphorescent Organic Light-Emitting Diodes. *Adv. Opt. Mater.* **2017**, *5*, 1600901.

(44) Kondakov, D. Y. *The Role of Homolytic Reactions in the Instrinsic Degradation of OLEDs*; So, F., Ed.; CRC Press: Boca Raton, FL, 2010; pp 211−242.

(45) Lee, J.; Jeong, C.; Batagoda, T.; Coburn, C.; Thompson, M. E.; Forrest, S. R. Hot Excited State Management for Long-Lived Blue Phosphorescent Organic Light-Emitting Diodes. *Nat. Commun.* **2017**, *8*, 15566.

(46) Schmidt, T. D.; Jäger, L.; Noguchi, Y.; Ishii, H.; Brütting, W. Analyzing Degradation Effects of Organic Light-Emitting Diodes via Transient Optical and Electrical Measurements. *J. Appl. Phys.* **2015**, *117*, 215502.

(47) Coehoorn, R.; van Eersel, H.; Bobbert, P.; Janssen, R. Kinetic Monte Carlo Study of the Sensitivity of OLED Efficiency and Lifetime to Materials Parameters. *Adv. Funct. Mater.* **2015**, *25*, 2024−2037.

(48) Jeon, S. K.; Lee, J. Y. Direct Monitoring of Recombination Zone Shift during Lifetime Measurement of Phosphorescent Organic Light-Emitting Diodes. *J. Ind. Eng. Chem.* **2015**, *32*, 332−335.